Neurochemistry International 56 (2010) 291–300

Contents lists available at ScienceDirect

Neurochemistry International

journal homepage: www.elsevier.com/locate/neuint

Critical role of lysosome and its associated protein cathepsin D in manganese-induced toxicity in cultured midbrain astrocyte

Xiaolan Fan [a,b,1], Guangrui Luo [a,1], Dehua Yang [a,1], Ming Ming [a], Hongmei Liu [a], Pu Pu [a], Weidong Le [a,c,*]

[a] The Key Laboratory of Stem Cell Biology, Institute of Health Sciences, Shanghai Institutes for Biological Sciences, Chinese Academy of Sciences & Shanghai Jiao Tong University School of Medicine Shanghai, 200025, PR China
[b] Fujian Medical University, Fuzhou, 350004, PR China
[c] Institute of Neurology, Ruijin Hospital, Jiao Tong University School of Medicine, Shanghai, 200025, PR China

ARTICLE INFO

Article history:
Received 15 November 2008
Received in revised form 25 October 2009
Accepted 2 November 2009
Available online 12 November 2009

Keywords:
Manganese
Apoptosis
Paraptosis
Lysosomes
Cathepsin D

ABSTRACT

Astrocyte is considered to be the initial target in manganese neurotoxicity; however, the ultra structure changes in the cells and the mechanism underlying the manganese-induced toxicity are still unclear. In this study, we conducted several assays in cultured midbrain astrocyte to determine the role of mitochondria, lysosome and its associated protein cathepsin D in the manganese-induced toxicity. We found that a mixed form of cell death in the manganese treated astrocyte. During the process of cell death, we detected extensive cytoplasmic vacuolation, mitochondrial swelling, and increased number and membrane permeability of lysosomes in the manganese treated astrocyte. Furthermore, we documented that after exposed to manganese, the Bax protein level in the astrocyte was increased, and its cellular distribution was significantly translocated from cytosol to mitochondria and lysosomes. Moreover, we demonstrated that manganese treatment caused significant increase of lysosomal enzyme cathepsin D, and pretreatment with cathepsin D inhibitor pepstatin A increased the apoptotic cell death. Collectively, our study suggests that different forms of cell death are involved in manganese-induced toxicity in the cultured midbrain astrocyte, and lysosome and its associated protein cathepsin D play a critical role in the pathological process. These results may shed new light on the mechanism of manganese exposure related neurological disorders.

1. Introduction

Manganese exposure is one of the important environmental risk factors for Parkinson's disease (Yokel, 2006). In central nervous system (CNS), reactive gliosis in response to manganese toxicity appears only in striatum and substantia nigra (Tomas-Camardiel et al., 2002). Glia including astrocyte, microglia and oligodendrocyte are all involved; but astrocyte is considered as the initial target in manganese-induced toxicity in the CNS (Henriksson and Tjalve, 2000).

Though both apoptosis and necrosis have been associated with the manganese-induced cell death in dopaminergic neurons (Desole et al., 1997; Latchoumycandane et al., 2005; Roth, 2006), only few studies referred to the cell death and mechanisms of manganese toxicity in astrocyte (Hazell et al., 1999).

The increase of oxidative stress, resulting from mitochondrial dysfunction in astrocyte, represents one of the key mechanisms by which manganese exerts its neurotoxicity (Hazell et al., 2006; Milatovic et al., 2007). Though most of the absorbed manganese in brain is deposited in mitochondria and lysosome-rich fractions, lysosomes take up manganese to a greater extent than mitochondria (Suzuki et al., 1983). It is hypothesized that manganese exposure may impair lysosomal functions and change the intracellular redox potential into oxidized state (Choi et al., 2002).

The total manganese levels in normal cerebral cortex are estimated to be 0.002–0.012 mM (Aschner et al., 1992, 1999; Wedler and Ley, 1994). Low concentrations of manganese (less than 0.01 mM) treatment for 24 h do not cause cell death (Chen and Liao, 2002) or any obvious morphological alteration (Rao and Norenberg, 2004) in cultured astrocyte. But higher concentrations of manganese (higher than 0.02 mM $MnCl_2$) can result in a time-dependent cell injury (Rama Rao et al., 2007). Here we choose both the low concentration (0.03 mM $MnCl_2$) and the high

* Corresponding author at: The Key Laboratory of Stem Cell Biology, Institute of Health Sciences, Shanghai Institutes for Biological Sciences, Chinese Academy of Sciences & Shanghai Jiao Tong University School of Medicine Shanghai, 200025, PR China. Tel.: +86 21 54669084; fax: +86 21 54669084.
E-mail address: wdle@sibs.ac.cn (W. Le).
[1] These authors contribute equally to this work.

0197-0186/$ – see front matter © 2009 Elsevier Ltd. All rights reserved.
doi:10.1016/j.neuint.2009.11.001

concentration (0.3 mM $MnCl_2$) of manganese to test the manganese-induced toxicity in cultured midbrain astrocyte.

In this study, we found three forms of cell death: apoptosis, necrosis and paraptosis in the cultured astrocyte after manganese exposure. We provided evidence that mitochondria and lysosomes were damaged in the manganese-induced toxicity, during which lysosomal enzyme cathepsin D and lysosomal membrane associated protein Bax might be the primary targets, and inhibition of cathepsin D can significantly enhance the manganese toxicity. Collectively, these results indicate that lysosome and its associated protein cathepsin D play a critical role in manganese-induced cell death in cultured midbrain astrocyte.

2. Materials and methods

2.1. Astrocyte cultures

Astrocyte was obtained from the mixed glia cultures as described previously (Liu et al., 2005) with some modification. Briefly, midbrain was isolated from 1-day-old BALB/c mice, dissociated with trypsin and cultured in DMEM-F12 (DF12) containing 10% new born calf serum (NCS), penicillin (50 U/ml; Gibco-BRL, USA) and streptomycin (50 μg/ml; Gibco-BRL, USA). Cells were plated in 75 ml tissue culture flasks at a density of 10^7 cells per flask and maintained at 37 °C in 5% CO_2. After confluence, the cultures were shaken to remove microglia and oligodendrocyte, and the adherent cells were allowed to grow for another 3 days. Then, flasks were shaken again under the same condition to remove the remaining microglia and oligodendrocyte; the remaining adherent cells were released with mild trypsination as reported (Saura et al., 2003) and reseeded. At least after four passages, astrocyte was zused in the subsequent experiments. Astrocyte purity was found >95% based on immunocytochemical staining of a specific astrocyte marker, glial fibrillary acidic protein (GFAP). Astrocytes were seeded at a density of 10^5 cells/cm^2 in 6 well (for Western blot) or on cover slips in 24 well (for cell staining) plastic tissue culture plates for 3 days and then the medium was replaced to the DF12 with 2% NCS. 48 h later, the cultures were treated with low or high concentrations of manganese chloride ($MnCl_2$, Sigma, USA). Lysosomal enzyme cathepsin D inhibitor Pepstatin A (Merck, Germany) was pre-incubated for 24 h and then co-cultured with manganese in the astrocyte. After 2–72 h culture, the cells were harvested to extract RNA for real-time reverse transcription polymerase chain reaction (RT-PCR) analysis, to extract protein for Western blot assay or processed for cell staining.

2.2. Propidium iodide (PI) and 4′,6-diamidino-2-phenylindole (DAPI) staining

PI and DAPI were used to stain DNA in the nuclei. Briefly, cells cultured on cover glasses were gently washed twice with phosphate-buffered saline (PBS) and incubated with 5 μg/ml PI (Sigma, USA) and DAPI (Biotium, USA) for 30 min. The cells were then washed with PBS and nuclear fluorescence was detected using a fluorescence microscope equipped with DP70 CCD digital camera (Olympus IX81, Japan) with the 488 nm filter of an Argon-ion laser for excitation.

2.3. LysoTracker® and MitoTracker® dyes staining

LysoTracker® dyes (50 nM, Invitrogen, USA) were used to stain lysosomes and MitoTracker® dyes (50 nM, Invitrogen, USA) were used to stain mitochondria according to the product's instruction. Astrocyte cultures on cover slips of 24-well-dish were incubated for 0.5 h with the pre-warmed (37 °C) LysoTracker Red DND-99-containing medium or MitoTracker® containing medium. Then the loading solution was replaced with fresh medium and the cells were photographed. The absorption wave is 577 nm and the emission wave is 599 nm.

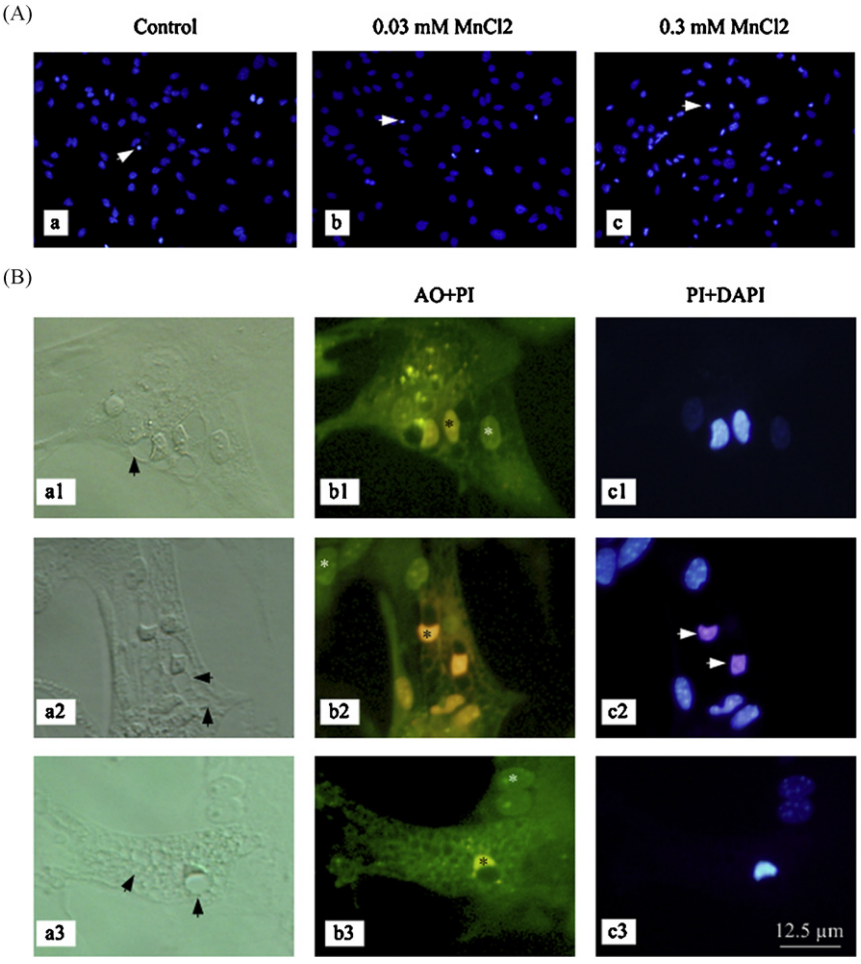

Fig. 1. Manganese-induced cell death in astrocyte detected by DAPI and AO-PI. (A) DAPI staining of the nuclei in the control astrocyte (a), in the astrocyte with 0.03 mM $MnCl_2$ treatment for 24 h (b), in the astrocyte with 0.3 mM $MnCl_2$ treatment for 24 h (c); white arrows indicate the densely stained nuclei. (B) Staining pattern of semi-moon-like nuclei in the astrocyte treated with 0.3 mM $MnCl_2$ for 24 h. Changes in number and size of vacuoles (black arrows) were observed under light microscope (a1–a3). Nuclei were stained with AO-PI; AO stained nuclei in green (white asterisk), PI stained nuclei in red (black asterisk), (b1–b3). Nuclei were stained with PI and DAPI showing that some densely DAPI-stained nuclei were PI positive (c1–c3, white arrows).

2.4. Acridine orange (AO) and 5,5′,6,6′-tetrachloro-1,1′,3,3′-tetraethylbenzimidazolyl-carbocyanine iodide (JC-1) staining

AO and JC-1 were used in the cultured astrocyte to detect the membrane integrity of lysosomes and mitochondria, respectively. AO (5 mg/ml PBS, Sigma, USA) or JC-1 (5 mg/ml, Beyotime, China) were added to the cultured astrocytes to a final concentration of 5 μg/ml for 15 min under standard culture conditions and then washed with pre-warmed fresh medium. The relative intensities of red and green fluorescence were simultaneously examined microscopically. The absorption wave was 490 nm and the emission wave was 590 nm.

2.5. Immunofluorescent staining

For immunofluorescent staining, cells were washed three times in D-Hanks' and then fixed for 15 min at 37 °C in 4% PFA. After incubation with PBS containing 0.2% Triton X-100, 5% bovine serum albumin (BSA) for 30 min at room temperature (RT), the cells were incubated with primary antibody (Bax, 1:500, sc-493, Santa Cruz Biotechnology, USA; cathepsin D, 1:500, sc-10725, Santa Cruz Biotechnology, USA; cleaved caspase-3, 1:200 #9661, Cell Signaling, USA) overnight at 4 °C; after washing, the cells were then incubated with secondary antibody (Cy2-conjugated anti-rabbit IgG, 1:200, Jackson, USA) at RT for 2 h; and finally nuclear DNA was stained with DAPI in PBS at RT for 1 min.

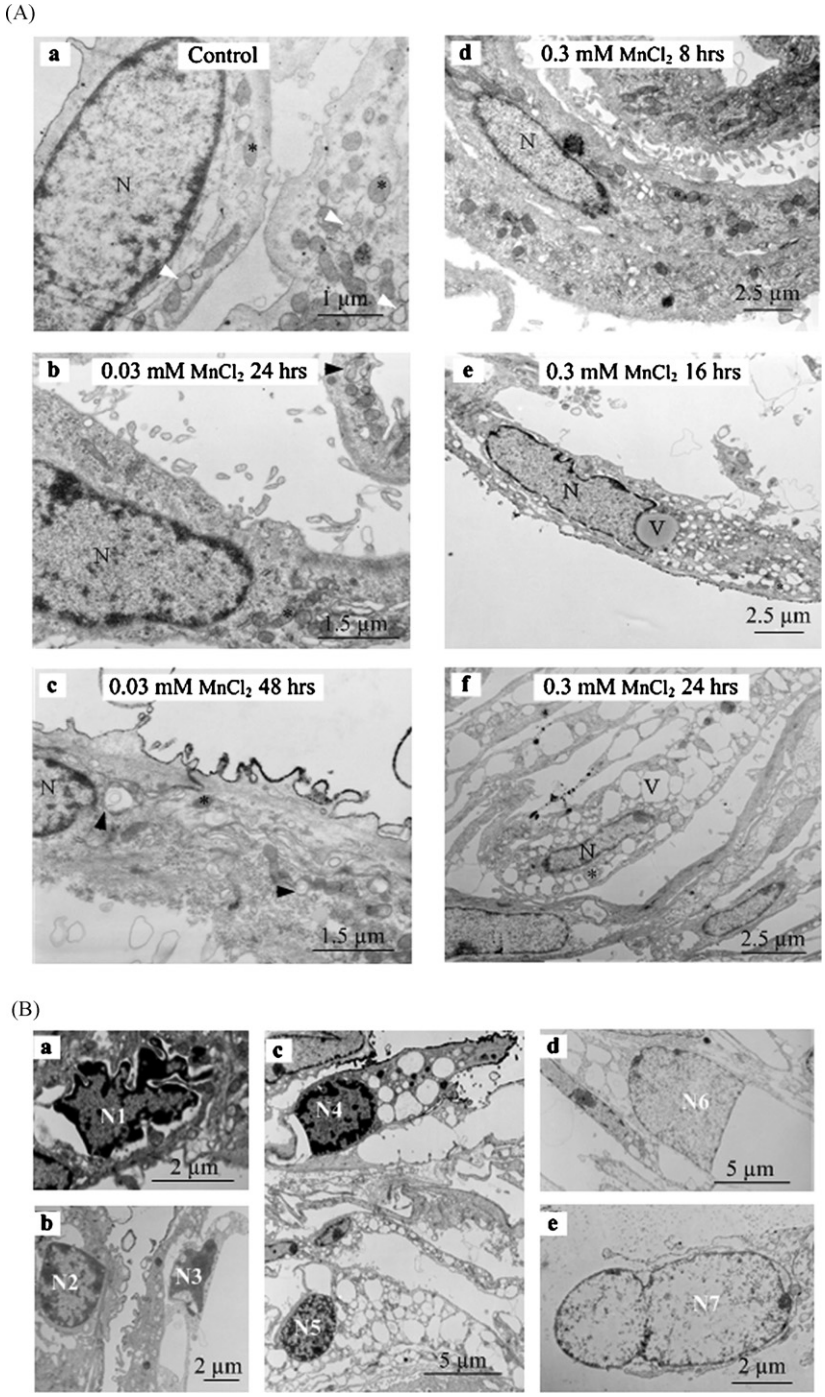

Fig. 2. TEM observation in manganese treated astrocyte. (A) Mitochondrial swelling, condensation of the mitochondrial matrix, cytoplasmic lucency and vacuolization and polyribosomal disaggregation were seen in the cytoplasm. Control astrocyte (a). Astrocyte treated with 0.03 mM $MnCl_2$ for 24 h showing two layer membrane structure with dense content (b, black arrow), while astrocyte treated with 0.03 mM $MnCl_2$ for 48 h showing that the dense content in the two membrane structure was much less or disappeared (c, black arrow). We hardly saw any two layer membrane structure in astrocyte with 0.3 mM $MnCl_2$ treatment for 8 h (d), 16 h (e) or 24 h (f). Instead, we observed lot of vacuoles surrounded by one layer membrane with or without contents inside. *: Mitochondrion, N: nucleus, V: vacuole, white arrow: ER, black arrow: AV. (B) Nuclear morphology of astrocyte treated with 0.3 mM $MnCl_2$ for 16–24 h showing heterochromatin condensed in discrete clumps in cell without vacuole (a: N1, b: N2) and in cell with vacuole (b: N3, c: N4), chromatin clustering to loose speckles in cell with vacuoles (c: N5, d: N6), and cell membrane ruptured with only nucleus left (e: N7).

2.6. Quantitative real-time RT-PCR measurements of gene expression

Primers for cathepsin D were designed as follows: forward, 5-GTTAA-CAACGTGCTTCCGGTCTT-3; reverse, 5-GCCACCAAGCATTAGTTCTCCT C-3 (Sangon Biotech, Inc., Shanghai, China). Real-time PCR was performed by Chromo 4 Sequence Detection System (Bio-Rad, Inc., Hercules, CA, USA) utilizing a SYBR Green PCR premix reagent (TOYOBO, Inc., Japan). The PCR reaction was set up as follows: initial denaturation at 95 °C for 10 min, followed by 40 cycles of 15 s at 95 °C, 15 s at 58 °C and 30 s at 72 °C. The levels of cathepsin D expression were normalized to GAPDH for which the primers were designed as follows: forward, 5-CCATGTTTGT-GATGGGTGTGA ACCA-3; reverse, 5-ACCAGTGGATGCAG GGATGATGTTC-3.

2.7. Western blot assay

For Western blot assay, cells were washed three times with cold PBS, and then harvested with a cell scraper, and lysed in cold lysis buffer (modified RIPA) after centrifugation. An aliquot (25–40 μg protein) of the supernatant was loaded onto an SDS–polyacrylamide gel (12%). After transferred to PVDF membrane, the separated proteins on the membrane were incubated with antibody. The primary antibodies used here were cathepsin D (1:500, sc-10725, Santa Cruz Biotechnology, USA), cathepsin D (C-20): (1:500, sc-6486, Santa Cruz Biotechnology, USA), Bax (1:1000, Cell Signaling, USA) and actin (1:4000, Sigma, USA) as loading control; the membrane was continuously incubated with appropriate secondary antibodies coupled to horseradish peroxidase, and then developed with enhanced chemiluminescence (ECL) substrate (Supersignal West Dura Extended Duration Substrate, Pierce, USA).

2.8. Lysosomes isolation

The procedure of primary astrocyte culture and drug treatment was the same as described above. About 1.0×10^8 cells of the control astrocyte and the 0.3 mM $MnCl_2$ treated astrocyte were harvested and manipulated according to the manufacture's instruction (Lysosomal Isolation Kit, Sigma, USA). Briefly, the harvested cells were broken by the homogenizer in the lyses buffer to an 80% of the cell breakage degree determined by Trypan Blue staining. After the centrifugation at $1000 \times g$ for 10 min, the pellet with cell fragmentation was discarded and the supernatant was centrifuged again at $20{,}000 \times g$ for 20 min. Then the supernatant was collected as the cytoplasmic fraction and the pellet was re-suspended which is called Crude Lysosomal Fraction (CLF). CLF was separated by density gradient centrifugation at $150{,}000 \times g$ for 4 h and the further purified lysosomal fraction was collected. The protein lysis of the lysosomal fraction was quantified by Bradford assay.

2.9. Transmission electron microscopy (TEM) examination

To perform the TEM examination in the cultured astrocyte, the medium in the culture wells was removed followed by washing with PBS; the cells were then fixed in 0.1 M sodium phosphate buffer (PBS) containing 2.5% glutaraldehyde and 1% OsO_4 (pH 7.2–7.4) for 12 h. After that the cells were embedded into Ultracut and sliced into 60 nm sections which were stained with uranyl acetate and lead citrate, and examined in TEM (Philips CM-120, The Netherlands).

2.10. Statistical analysis

Significant differences between experimental groups were determined using one-way ANOVA with Excel. P value of less than 0.05 was considered to have significant difference. The quantitative data were obtained from 3 to 4 independent assays with duplication in each assay.

3. Results

3.1. Multiple forms of cell death were observed in the astrocyte treated with manganese

Cells with dense DAPI-stained nuclei were traditionally considered as being in the process of apoptosis; so we applied DAPI staining to detect the level of apoptosis in manganese treated astrocyte. We found that there were only a few densely DAPI-stained nuclei (<7%) in the untreated or 24 h 0.03 mM $MnCl_2$ treated astrocyte, but the number of densely DAPI-stained nuclei was dramatically increased (nearly 38%) in astrocyte exposed to 0.3 mM $MnCl_2$ (Fig. 1A, white arrow). By bright field microscope, we observed a few cells (about 8%) having semi-moon-like nuclei with a large vacuole nearby in 0.3 mM $MnCl_2$ but not in 0.03 mM $MnCl_2$ treated astrocyte (Fig. 1B, black arrow). In these cells, vacuoles were distributed more or less in the cytoplasm. We stained these cells with AO-PI and DAPI (Fig. 1B, b1–b3, c1–c3). AO stained green in nuclei when the cells were healthy while PI stained red in nuclei when the cells were undergoing late process of apoptosis or necrosis. It was shown that almost all these semi-moon-like nuclei were densely DAPI-stained, but only a few (around 20%) were PI-stained, which suggest that a majority of cells with semi-moon-like nuclei may undergo apoptosis and a minority of the cells may suffer from necrosis.

Furthermore, we observed the changes of mitochondrial swelling, mitochondrial matrix condensation, cytoplasmic lucency and vacuolization, and polyribosomal clusters disaggregation by TEM (Fig. 2A, b–f). In addition, we detected the increased autophagy vacuoles (AVs), the two-layer membrane structures with high density content inside in astrocyte after the treatment of 0.03 mM $MnCl_2$ for 24 h (Fig. 2A, b, black arrowhead). When the treatment of 0.03 mM $MnCl_2$ extended to 48 h, the density of the content inside AVs was decreased (Fig. 2A, c, black arrowheads). Compared to that, we observed lots of vacuoles surrounded by one layer membrane with low density or none content inside instead of

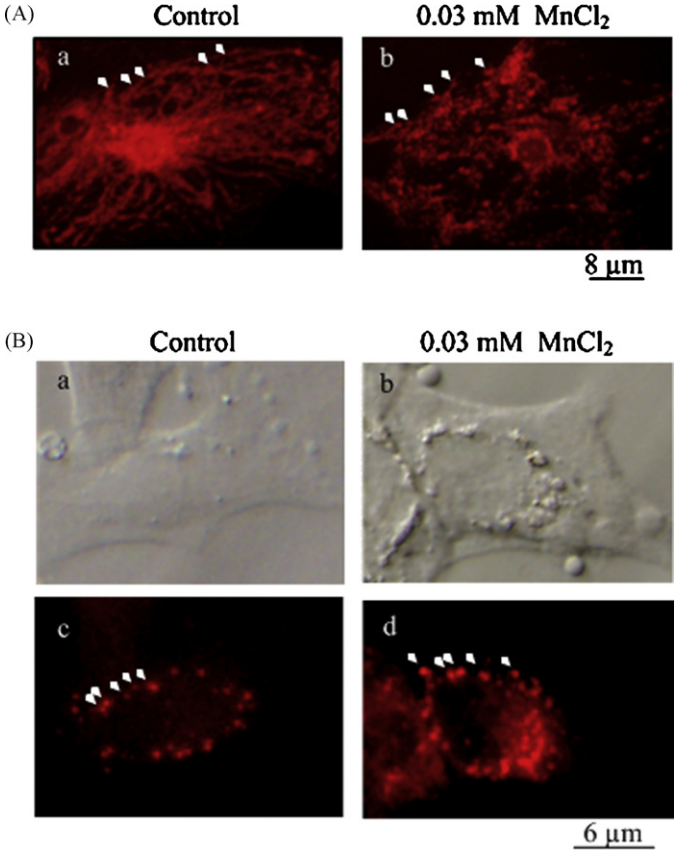

Fig. 3. Mitochondrial and lysosomal damage in astrocyte after manganese exposure. (A) Mitochondria with MitoTracker staining. The red fluorescence dots (white arrows) marked the mitochondria. The number of mitochondria in the astrocyte treated with 0.03 mM $MnCl_2$ for 24 h was decreased and the mitochondria were disorganized (b) as compared to those of control (a). (B) The upper lane (a, b) was the observation under light microscope of the same field of the LysoTracker staining (c, d). The red fluorescence dots (white arrows) marked the lysosomes which were increased in the astrocyte treated with 0.03 mM $MnCl_2$ for 24 h (d) as compared to those of control (c). (C) Mitochondria function was detected by JC-1 staining (a1–a4) and the lysosomal membrane stability was determined by AO staining. Photos were taken after 2 s (b1–b4) and 12 s (c1–c4) of exposure to the excitation light in astrocyte treated with 0.3 mM $MnCl_2$ for 4 h, 18 h and 28 h, separately. The red fluorescence was decreased while the green fluorescence was increased in both JC-1 staining and AO staining after manganese exposure. (For interpretation of the references to colour in this figure legend, the reader is referred to the web version of the article.)

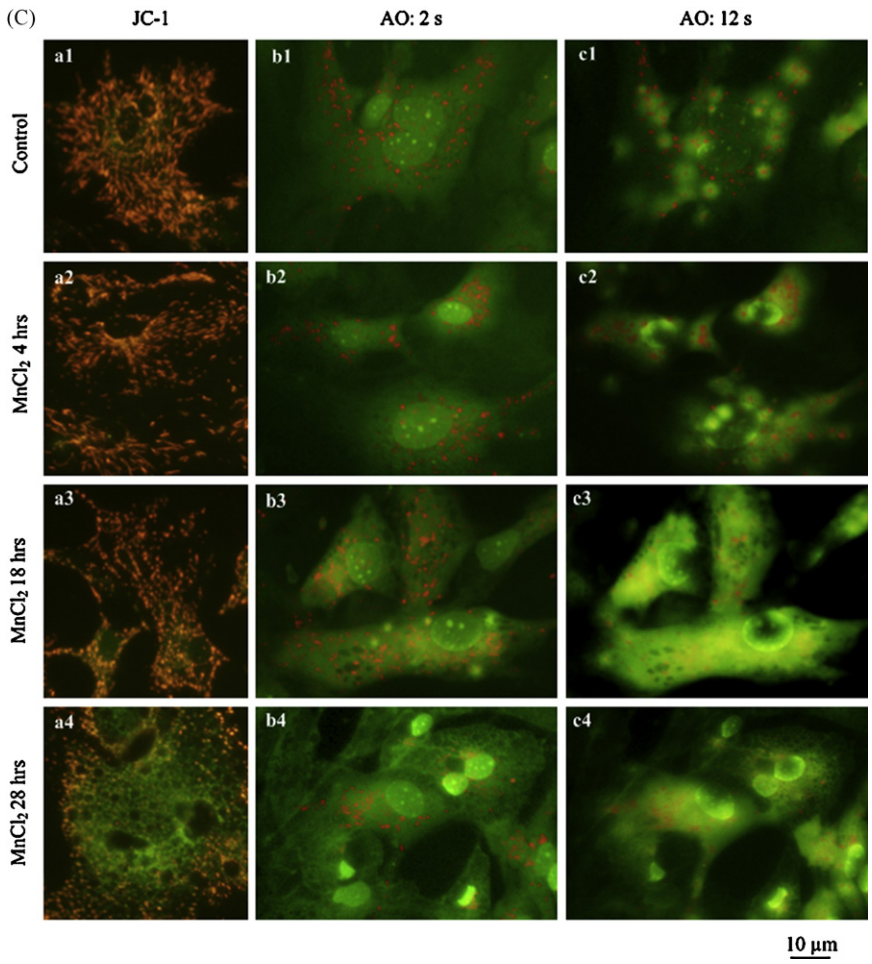

Fig. 3. (*Continued*).

AVs in astrocyte with 0.3 mM $MnCl_2$ treatment for 8 h, 16 h or 24 h (Fig. 2A, d–f). In these astrocyte, the nuclear morphology with characteristic of apoptosis (heterochromatin condensed in discrete clumps; Fig. 2B, N3 and N4), paraptosis (no chromatin condensation but at best, chromatin clustering to loose speckles; Fig. 2B, N5 and N6), or necrosis (cytoplasmic swelling and cell membrane rupture) were observed (Fig. 2B, N7).

3.2. Mitochondrial and lysosomal damage in manganese treated astrocyte

Mitochondria and lysosomes are two important cell organelles involved in cell death. Mitochondrial damage was reported in manganese toxicity in astrocyte (Rao and Norenberg, 2004; Tjalkens et al., 2006; Yin et al., 2008), but none was reported of the lysosomal damage in manganese treated astrocyte. Using MitoTracker dyes to detect manganese-induced mitochondrial damage, we found that the number of mitochondria stained by MitoTracker dyes was decreased and its morphology seemed disorganized as compared with the control astrocyte (Fig. 3A). Contrary to the change in mitochondria, the number of lysosomes, which appeared as dot-like red fluorescence by LysoTracker dyes, was increased and the volume of each dot was becoming larger in manganese treated astrocyte than that in control astrocyte (Fig. 3B, white arrows). Moreover, we further confirmed the manganese-induced damage of mitochondrial membrane integrity by JC-1 dye staining, which was accumulated as aggregates with red fluorescence in healthy mitochondria (Fig. 3C, a1). We observed a significant change in JC-1 staining in the astrocyte after 0.3 mM $MnCl_2$ treatment for 24 h (Fig. 3C, a4). The longer time the cells were under manganese treatment, the less JC-1 dye was accumulated in the mitochondria; instead it stayed in the cytoplasm in a monomeric form with green fluorescence resulting from mitochondrial potential collapse (Fig. 3C, left lane). Moreover, we measured the lysosomal membrane stability by AO staining and found that the granular red fluorescence in the astrocyte was decreased after $MnCl_2$ treatment (Fig. 3C, middle and right lane), suggesting a significant damage to lysosomal membrane in addition to the mitochondrial membrane in the manganese exposed astrocyte.

3.3. Bax protein level was increased and it was co-localized with the makers of mitochondria and lysosomes in manganese treated astrocyte

Our results above implicate that the membrane permeability might be altered in mitochondria and lysosomes in the manganese treated astrocyte. Bax is a protein related to membrane permeability of both mitochondria and lysosomes. In order to investigate whether Bax is involved in the manganese toxicity in astrocyte, we measured the level of Bax protein and found an increase of Bax level in the astrocyte treated by 0.3 mM $MnCl_2$ (Fig. 4A); low concentration of manganese (0.03 mM $MnCl_2$) treatment in the cultured astrocyte had no obvious effect on Bax level (Fig. 4A). Using immunofluorescent staining, we found that Bax was almost equally distributed in the cytoplasm of control astrocyte, however, the Bax staining became denser and was intent to colocalize with the LysoTracker-stained lysosomes in the manganese treated

astrocyte (Fig. 4B and C). We also detected the Bax in the lysosomal fragment of the 0.3 mM $MnCl_2$ treated astrocyte and saw a moderate increase of the protein level (Fig. 5D).

3.4. Manganese treatment caused the changes in cathepsin D levels and its protein dislocation in astrocyte

Cathepsin D is a lysosomal proteinase. There are several forms of cathepsin D including the precursor (immature, inactive, 52 kDa), the intermediate (48 kDa) and the mature form (mature, active, 34 kDa and 14 kDa dimmer). In general, the mature forms of cathepsin D are located at lysosome while the premature forms of cathepsin D are outside of lysosome. In our experiment, the cathepsin D antibody (sc-10725) is able to detect the precursor (52 kDa) and the intermediate form (48 kDa) but difficult to detect the mature form (34 kDa) in Western blot downloaded with a total cellular protein preparation. Therefore, we combined both the premature 52 kDa and 48 kDa bands as the sum of premature

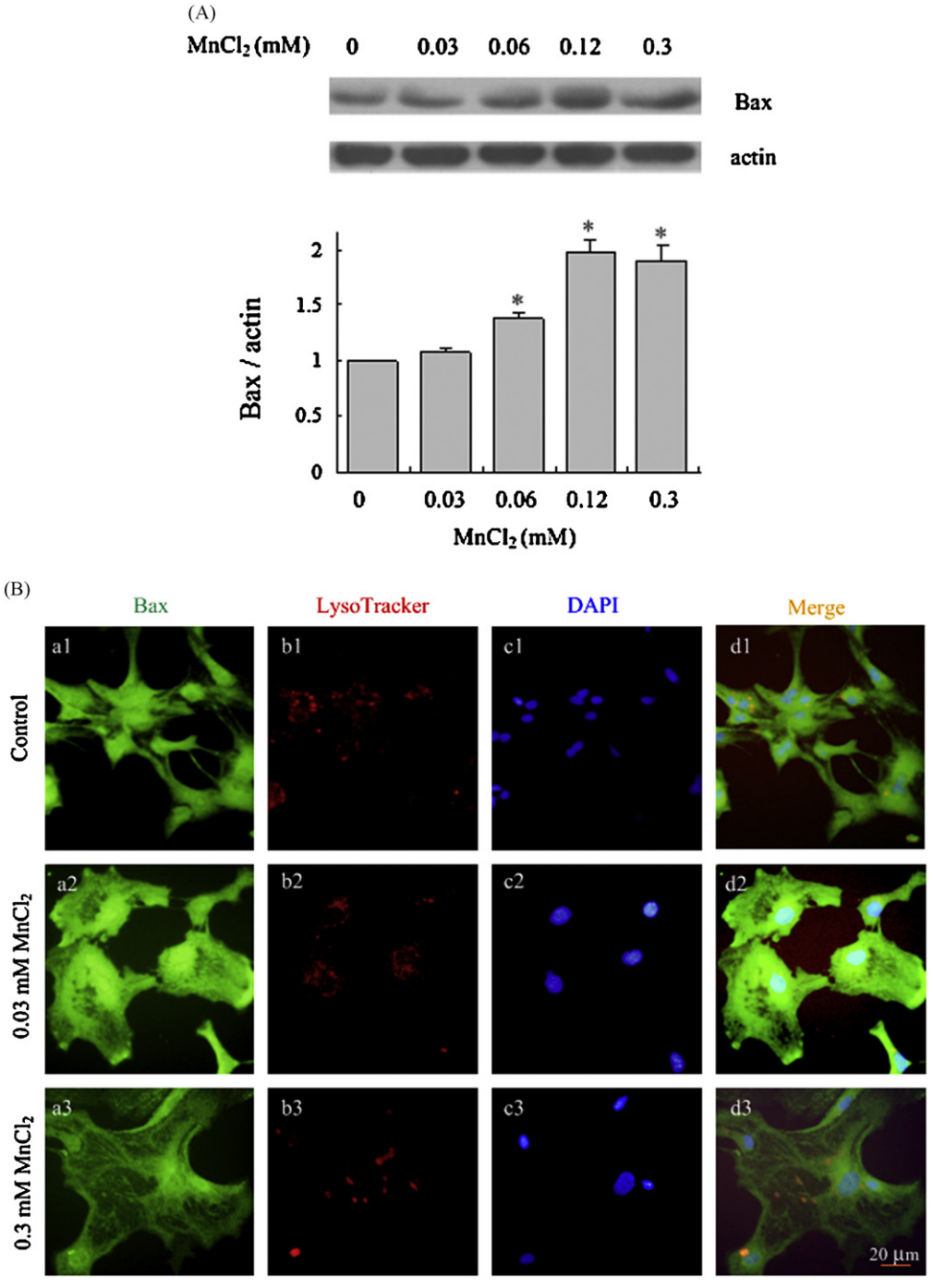

Fig. 4. Bax expression and its distribution in astrocyte treated with manganese. (A) Western blot and quantitative analysis of Bax expression in manganese treated astrocyte showed that total Bax protein level was elevated by 0.06–0.3 mM $MnCl_2$ exposure for 24 h, $^*p < 0.05$ versus control. (B and C) Bax staining (a1–a3) with LysoTracker staining (b1–b3 in B) or MitoTracker staining (b1–b3 in C) showed that Bax (green) was distributed uniformly in the cytosol (a1). Nuclei were stained with DAPI (c1–c3) and the merged results were shown in d1–d3. After the indicated time and concentration of manganese treatment, Bax was distributed in a dot like pattern in the manganese treated astrocyte (a2 and a3) and it was co-localized with the LysoTracker-stained lysosomes (red, B) and MitoTracker-stained mitochondria (red, C). (For interpretation of the references to colour in this figure legend, the reader is referred to the web version of the article.)

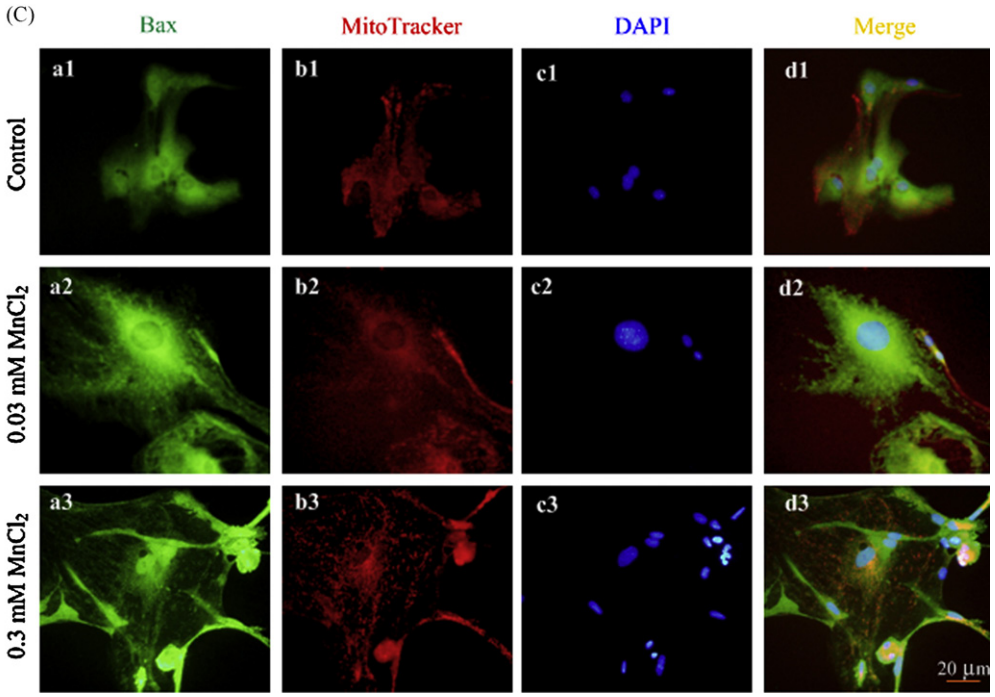

Fig. 4. (*Continued*).

cathepsin D for the statistic analysis. We found that the protein levels of premature cathepsin D were increased after the manganese exposure in a dose-dependent manner (Fig. 5A). In addition, we detected significantly higher mRNA expression levels after manganese treatment with the peak at 2 h (Fig. 5B). The immunofluorescent staining showed that cathepsin D was distributed in a dot like pattern in the control cells; however, in manganese treated astrocyte, it was distributed uniformly in the cytosol (Fig. 5C). Further, in both the lysosomal fraction and the cytoplasmic fraction of astrocyte with manganese treatment, we detected the significantly higher levels of premature (52 kDa and 48 kDa) and mature forms of cathepsin D (34 kDa) (Fig. 5D).

3.5. Pretreatment of cathepsin D inhibitor pepstatin A increased apoptosis and decreased premature cathepsin D protein levels in the manganese treated astrocyte

We counted cell apoptosis by DAPI staining (Fig. 6A), and found that 0.03 mM manganese treatment did not significantly affect the number of apoptotic cells, while 0.3 mM manganese treatment markedly increased the apoptotic cells by 33%. As cathepsin D was increased in a dose-dependent manner in astrocyte after manganese treatment, we further investigated the role of cathepsin D in the manganese-induced toxicity. Pretreatment with pepstatin A significant increased apoptotic cells by 45% with the detection of DAPI staining (Fig. 6A) as well as the cleaved caspase-3 staining (B), whereas pepstatin A pretreatment decreased the protein levels of premature cathepsin D (C).

4. Discussion

4.1. Multiple forms of cell death and organelles dysfunction are involved in manganese-induced toxicity in astrocyte

In addition to the recent report that apoptosis is a major form of cell death presented in manganese treated astrocyte (Gonzalez et al., 2008), we have identified two other forms of cell death, necrosis and paraptosis, in the manganese treated astrocyte. Before the cell death occurs we have found a significant alteration of mitochondria and lysosomes in the astrocyte following manganese-induced toxicity. Further, we have detected a significant amount of vacuoles in cells that underwent the process of apoptosis or paraptosis. Those vacuoles with light density substance may be lysosomes or degenerating mitochondria, and vacuoles without content may be the dilated endoplasmic reticulum (ER). The ERs and mitochondria are considered as two targeted organelles affected in the cells with extensive vacuoles characteristic of paraptosis (Hoa et al., 2007). Recently the mitochondrial impairment has been indicated in the manganese-induced apoptosis in astrocyte (Gonzalez et al., 2008). In our study, the lysosomal membrane damage is clearly seen in the astrocyte with high concentration of manganese treatment for 4 h whereas mitochondrial impairment is obviously detected in the astrocyte with the same treatment for 18 h (Fig. 3). Therefore we believe that the impairment in both lysosomes and mitochondria plays critical role in the manganese-induced cell death in astrocyte.

Moreover, we have observed abundant autophagic AVs but no obvious cell loss in the astrocyte treated with low concentration of manganese. It is known that under stress condition, AVs can be induced to protect the cells (Komatsu et al., 2007; Saka et al., 2007; Pallet et al., 2008; Sakiyama et al., 2009). However, for the acute mitochondrial and lysosomal impairment following high concentration of manganese treatment, the cells may not have enough time to induce AVs for the protection before death. Further investigation of the relationship among the different forms of cell deaths and the role of autophagy is needed to provide valuable information for the mechanisms of manganese-induced toxicity.

4.2. Critical role of cathepsin D in manganese-induced astrocyte apoptosis

Cathepsin D has been reported to be involved in caspase-independent cell death pathway in hair cells in vivo (Jiang et al., 2006) and leakage of cathepsin D to the cytosol after oxidative stress-induced lysosomal destabilization can act as a proapoptotic

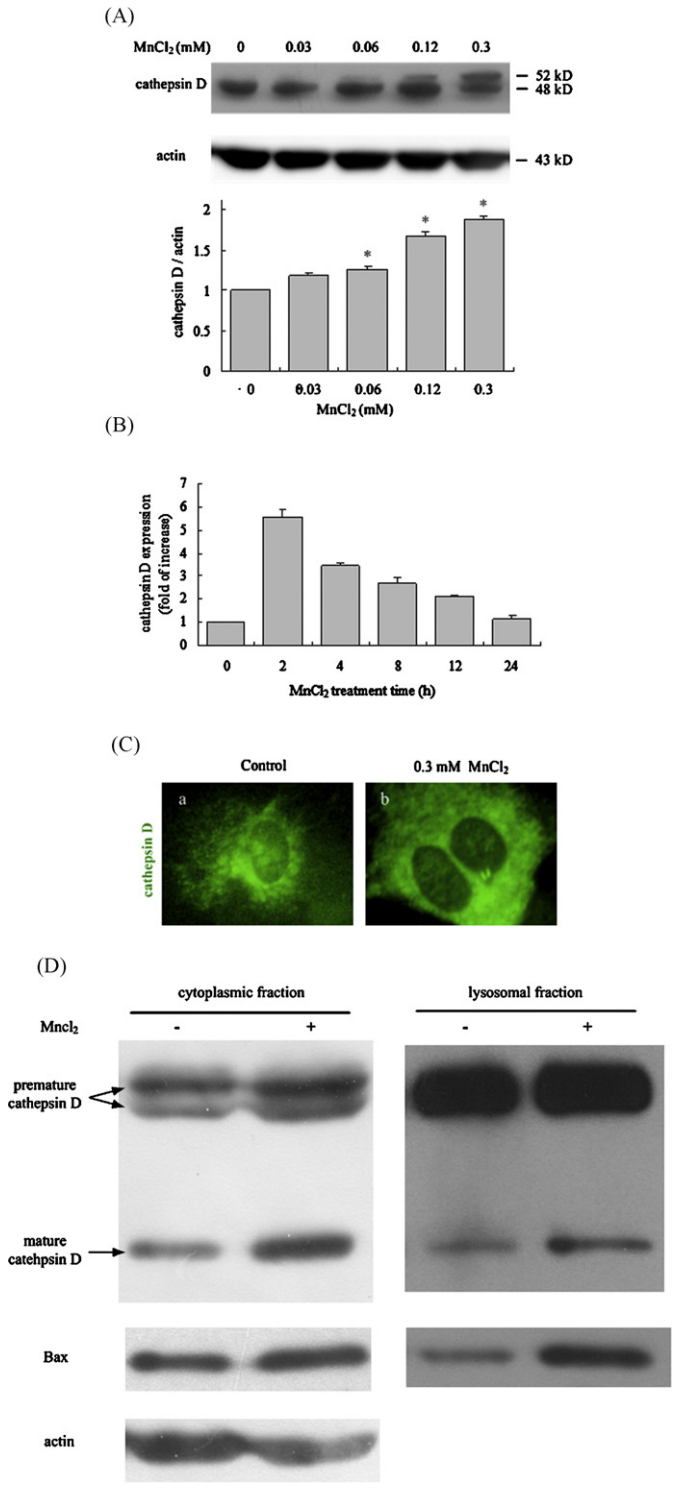

Fig. 5. Cathepsin D expression and its distribution in manganese treated astrocyte. (A) Western blot and quantitative analysis showed that cathepsin D expression was increased in a dose-dependent manner in astrocyte treated with manganese, $^{*}p < 0.05$ versus control. (B) A real-time PCR for the mRNA level in astrocyte treated with 0.3 mM $MnCl_2$ for 2 h, 4 h, 8 h, 12 h and 24 h. Expression of cathepsin D mRNA was normalized to that of GAPDH. Cathepsin D expression is increased after manganese treatment at all the detected time points, with the highest level at 2 h (more than 6-folds) and decreased at the sequential time points. (C) Immunofluorescent staining showed that cathepsin D was distributed in a dot like pattern in the control cells (a). After 0.3 mM $MnCl_2$ treatment for 24 h, cathepsin D was distributed uniformly in the cytosol (b). (D) Western blot of cathepsin D and Bax proteins in the lysosomal fraction and the cytoplasmic fraction. The mature form of cathepsin D (34 kDa) was found robustly increased while the premature form of cathepsin D was moderately increased in the both lysosomes and cytoplasmic fractions from astrocyte treated with manganese. The Bax was detected elevated in both fractions of manganese treated astrocyte. The figure represents results of two independent experiments.

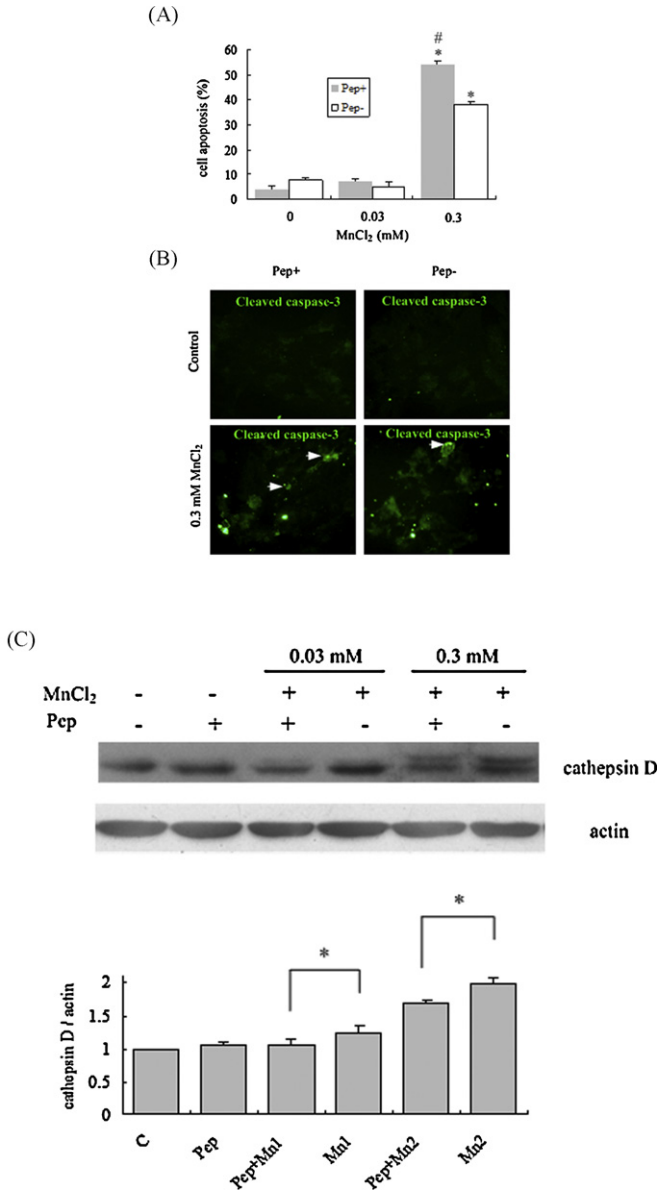

Fig. 6. Cathepsin D inhibitor pepstatin A increased apoptosis in manganese treated astrocyte. (A) DAPI staining showed there was almost no condensed DAPI dot in the control astrocyte or in the astrocyte treated with pepstatin A alone. 0.03 mM $MnCl_2$ treatment did not significantly affect the cell death. Pretreatment with pepstatin A significant increased the cell death after 0.3 mM $MnCl_2$ exposure for 24 h. The values were mean ± S.E. of three independent experiments, $^{*}p < 0.05$ versus control, $\#p < 0.05$ versus the same concentration of manganese treatment without pepstatin A pretreatment. Pep+: with 10 μM pepstatin A pretreatment. Pep−: without pepstatin A pretreatment. (B) Caspase-3 immunofluorescent staining (white arrows) showed that pepstatin A pretreatment increased the caspase-3 positive apoptotic cell number in the astrocyte treated with 0.3 mM $MnCl_2$. (C) Pepstatin A treatment decreased the protein level of cathepsin D in the manganese treated astrocyte. Mn1:0.03 mM $MnCl_2$, Mn2:0.3 mM $MnCl_2$.

mediator upstream of cytochrome *c* release and caspase activation (Choi et al., 2002; Roberg et al., 2002). However, other evidences suggest that cathepsin D may play an important role in disposing of oxidative modified mitochondria in the aging and degenerating nervous system (Chopra et al., 1997), and it can function as an antiapoptotic signaling in neuroblastoma cells (Sagulenko et al., 2008). The contradictory role of cathepsin D referred above may be

due to its distribution in cells which are affected by the membrane permeability of lysosomes.

It has been reported that activation of Bax can increase mitochondrial membrane permeability (Tan et al., 2006; Siu et al., 2008) and the insertion of Bax into the lysosomal membrane can change its permeability and induce the release of lysosomal enzymes (Kagedal et al., 2005; Werneburg et al., 2007). Based on the results from our study we propose that the dislocation of Bax to lysosomes rather than the protein level change in the manganese treated astrocyte may cause the change in the lysosomal membrane permeability in responding to manganese toxicity. The increased membrane permeability of lysosomes may result in the alternation of the cathepsin D distribution to the cytosol. Unlike most of the lysosomal enzymes that only function in acid lysosomal environment, cathepsin D is active both in the neutral pH cytosol and in the acid lysosomes (Banay-Schwartz et al., 1987; Bednarski and Lynch, 1996). Our results suggest that manganese exposure may cause leakage of the mature form of cathepsin D from lysosomes to cytosol and the decreased enzyme activity by pepstatin A may lead to more cell death.

Furthermore, there have been reports showing that cathepsin D in the cytosol can induce the conformational change of Bax and its insertion into the outer mitochondrial membrane (Laforge et al., 2007), and the cathepsin D activity is mandatory for the oligomerization of Bax on both mitochondrial and lysosomal membranes (Castino et al., 2008). However, it is unknown at present which is the first response, the Bax insertion or the leakage of the cathepsin D to the manganese-induced toxicity. The relationship between cathepsin D and Bax still needs further investigation.

Moreover, we have documented that pepstatin A, a synthesized inhibitor of cathepsin D, can decrease the cathepsin D (52 kDa and 48 kDa) expression. Pepstatin A can bind to pro-cathepsin D and inhibit its auto-activation (Hasilik et al., 1982). The decreased protein of the cathepsin D (52 kDa and 48 kDa) after pepstatin A pretreatment may be due to the feedback regulation in the cells.

It is intriguing to know that astrocyte is the initial target in manganese neurotoxicity and the cells are more vulnerable than neurons to manganese-induced toxicity (Rao and Norenberg, 2004). It is believed that in manganese-induced neurological disorders, the impaired astrocytes may lose their capacity to protect and provide trophic support to their interacting neurons; instead these astrocytes may release cytotoxic free radicals, excitoamino acid, and other harmful inflammatory molecules to induce injury and death to neurons and other cells (Hazell, 2002). As the result, the neurons in the globus palidus and the substantia nigra are preferentially degenerated leading to the manganese-induced Parkinsonism or other related neurological disorders (Ordonez-Librado et al., 2008; Stanwood et al., 2009).

In conclusion, we observed a time- and dose-dependent apoptotic, necrotic or paraptotic cell death in astrocyte after exposure to manganese. We demonstrate that lysosomes and mitochondria are targets of the manganese-induced toxicity. We document that Bax and lysosomal enzyme cathepsin D play critical roles in manganese-induced apoptosis in astrocyte. Our study on the role of lysosome and its associated protein cathepsin D in the manganese-induced astrocyte injury may shed new light on the mechanisms of manganese exposure related neurological disorders and may help search for the effective therapeutic targets for the treatment of these disorders.

Acknowledgments

This work was supported by the National Nature Science Foundation of China (No. 30730096), the National Basic Research Program of China from Chinese Science & Technology Commission (2007CB947904), and the Chinese Science and Technology Commission (863 project 2007AA02Z460).

References

Aschner, M., Gannon, M., Kimelberg, H.K., 1992. Manganese uptake and efflux in cultured rat astrocytes. J. Neurochem. 58, 730–735.
Aschner, M., Vrana, K.E., Zheng, W., 1999. Manganese uptake and distribution in the central nervous system (CNS). Neurotoxicology 20, 173–180.
Banay-Schwartz, M., Dahl, D., Hui, K.S., Lajtha, A., 1987. The breakdown of the individual neurofilament proteins by cathepsin D. Neurochem. Res. 12, 361–367.
Bednarski, E., Lynch, G., 1996. Cytosolic proteolysis of tau by cathepsin D in hippocampus following suppression of cathepsins B and L. J. Neurochem. 67, 1846–1855.
Castino, R., Peracchio, C., Salini, A., Nicotra, G., Trincheri, N.F., Demoz, M., Valente, G., Isidoro, C., 2008. Chemotherapy drug response in ovarian cancer cells strictly depends on a cathepsin D-Bax activation loop. J. Cell Mol. Med..
Chen, C.J., Liao, S.L., 2002. Oxidative stress involves in astrocytic alterations induced by manganese. Exp. Neurol. 175, 216–225.
Choi, S.H., Choi, D.H., Lee, J.J., Park, M.S., Chun, B.G., 2002. Imidazoline drugs stabilize lysosomes and inhibit oxidative cytotoxicity in astrocytes. Free Radic. Biol. Med. 32, 394–405.
Chopra, V.S., Moozar, K.L., Mehindate, K., Schipper, H.M., 1997. A cellular stress model for the differential expression of glial lysosomal cathepsins in the aging nervous system. Exp. Neurol. 147, 221–228.
Desole, M.S., Sciola, L., Delogu, M.R., Sircana, S., Migheli, R., Miele, E., 1997. Role of oxidative stress in the manganese and 1-methyl-4-(2′-ethylphenyl)-1,2,3,6-tetrahydropyridine-induced apoptosis in PC12 cells. Neurochem. Int. 31, 169–176.
Gonzalez, L.E., Juknat, A.A., Venosa, A.J., Verrengia, N., Kotler, M.L., 2008. Manganese activates the mitochondrial apoptotic pathway in rat astrocytes by modulating the expression of proteins of the Bcl-2 family. Neurochem. Int. 53, 408–415.
Hasilik, A., von Figura, K., Conzelmann, E., Nehrkorn, H., Sandhoff, K., 1982. Lysosomal enzyme precursors in human fibroblasts. Activation of cathepsin D precursor in vitro and activity of beta-hexosaminidase A precursor towards ganglioside GM2. Eur. J. Biochem. 125, 317–321.
Hazell, A.S., 2002. Astrocytes and manganese neurotoxicity. Neurochem. Int. 41, 271–277.
Hazell, A.S., Desjardins, P., Butterworth, R.F., 1999. Increased expression of glyceraldehyde-3-phosphate dehydrogenase in cultured astrocytes following exposure to manganese. Neurochem. Int. 35, 11–17.
Hazell, A.S., Normandin, L., Norenberg, M.D., Kennedy, G., Yi, J.H., 2006. Alzheimer type II astrocytic changes following sub-acute exposure to manganese and its prevention by antioxidant treatment. Neurosci. Lett. 396, 167–171.
Henriksson, J., Tjalve, H., 2000. Manganese taken up into the CNS via the olfactory pathway in rats affects astrocytes. Toxicol. Sci. 55, 392–398.
Hoa, N.T., Zhang, J.G., Delgado, C.L., Myers, M.P., Callahan, L.L., Vandeusen, G., Schiltz, P.M., Wepsic, H.T., Jadus, M.R., 2007. Human monocytes kill M-CSF-expressing glioma cells by BK channel activation. Lab Invest. 87, 115–129.
Jiang, H., Sha, S.H., Forge, A., Schacht, J., 2006. Caspase-independent pathways of hair cell death induced by kanamycin in vivo. Cell Death Differ. 13, 20–30.
Kagedal, K., Johansson, A.C., Johansson, U., Heimlich, G., Roberg, K., Wang, N.S., Jurgensmeier, J.M., Ollinger, K., 2005. Lysosomal membrane permeabilization during apoptosis—involvement of Bax? Int. J. Exp. Pathol. 86, 309–321.
Komatsu, M., Wang, Q.J., Holstein, G.R., Friedrich Jr., V.L., Iwata, J., Kominami, E., Chait, B.T., Tanaka, K., Yue, Z., 2007. Essential role for autophagy protein Atg7 in the maintenance of axonal homeostasis and the prevention of axonal degeneration. Proc. Natl. Acad. Sci. U.S.A. 104, 14489–14494.
Laforge, M., Petit, F., Estaquier, J., Senik, A., 2007. Commitment to apoptosis in CD4(+) T lymphocytes productively infected with human immunodeficiency virus type 1 is initiated by lysosomal membrane permeabilization, itself induced by the isolated expression of the viral protein Nef. J. Virol. 81, 11426–11440.
Latchoumycandane, C., Anantharam, V., Kitazawa, M., Yang, Y., Kanthasamy, A., Kanthasamy, A.G., 2005. Protein kinase Cdelta is a key downstream mediator of manganese-induced apoptosis in dopaminergic neuronal cells. J. Pharmacol. Exp. Ther. 313, 46–55.
Liu, X., Fan, X.L., Zhao, Y., Luo, G.R., Li, X.P., Li, R., Le, W.D., 2005. Estrogen provides neuroprotection against activated microglia-induced dopaminergic neuronal injury through both estrogen receptor-alpha and estrogen receptor-beta in microglia. J. Neurosci. Res. 81, 653–665.
Milatovic, D., Yin, Z., Gupta, R.C., Sidoryk, M., Albrecht, J., Aschner, J.L., Aschner, M., 2007. Manganese induces oxidative impairment in cultured rat astrocytes. Toxicol. Sci. 98, 198–205.
Ordonez-Librado, J.L., Gutierrez-Valdez, A.L., Colin-Barenque, L., Anaya-Martinez, V., Diaz-Bech, P., Avila-Costa, M.R., 2008. Inhalation of divalent and trivalent manganese mixture induces a Parkinson's disease model: immunocytochemical and behavioral evidences. Neuroscience 155, 7–16.
Pallet, N., Bouvier, N., Legendre, C., Gilleron, J., Codogno, P., Beaune, P., Thervet, E., Anglicheau, D., 2008. Autophagy protects renal tubular cells against cyclosporine toxicity. Autophagy 4, 783–791.
Rama Rao, K.V., Reddy, P.V., Hazell, A.S., Norenberg, M.D., 2007. Manganese induces cell swelling in cultured astrocytes. Neurotoxicology 28, 807–812.

Rao, K.V., Norenberg, M.D., 2004. Manganese induces the mitochondrial permeability transition in cultured astrocytes. J. Biol. Chem. 279, 32333–32338.
Roberg, K., Kagedal, K., Ollinger, K., 2002. Microinjection of cathepsin d induces caspase-dependent apoptosis in fibroblasts. Am. J. Pathol. 161, 89–96.
Roth, J.A., 2006. Homeostatic and toxic mechanisms regulating manganese uptake, retention, and elimination. Biol. Res. 39, 45–57.
Sagulenko, V., Muth, D., Sagulenko, E., Paffhausen, T., Schwab, M., Westermann, F., 2008. Cathepsin D protects human neuroblastoma cells from doxorubicin-induced cell death. Carcinogenesis 29, 1869–1877.
Saka, H.A., Gutierrez, M.G., Bocco, J.L., Colombo, M.I., 2007. The autophagic pathway: a cell survival strategy against the bacterial pore-forming toxin Vibrio cholerae cytolysin. Autophagy 3, 363–365.
Sakiyama, T., Musch, M.W., Ropeleski, M.J., Tsubouchi, H., Chang, E.B., 2009. Glutamine increases autophagy under Basal and stressed conditions in intestinal epithelial cells. Gastroenterology 136, 924–932.
Saura, J., Tusell, J.M., Serratosa, J., 2003. High-yield isolation of murine microglia by mild trypsinization. Glia 44, 183–189.
Siu, W.P., Pun, P.B., Latchoumycandane, C., Boelsterli, U.A., 2008. Bax-mediated mitochondrial outer membrane permeabilization (MOMP), distinct from the mitochondrial permeability transition, is a key mechanism in diclofenac-induced hepatocyte injury: multiple protective roles of cyclosporin A. Toxicol. Appl. Pharmacol. 227, 451–461.
Stanwood, G.D., Leitch, D.B., Savchenko, V., Wu, J., Fitsanakis, V.A., Anderson, D.J., Stankowski, J.N., Aschner, M., McLaughlin, B., 2009. Manganese exposure is cytotoxic and alters dopaminergic and GABAergic neurons within the basal ganglia. J. Neurochem. 110, 378–389.
Suzuki, H., Wada, O., Inoue, K., Tosaka, H., Ono, T., 1983. Role of brain lysosomes in the development of manganese toxicity in mice. Toxicol. Appl. Pharmacol. 71, 422–429.
Tan, C., Dlugosz, P.J., Peng, J., Zhang, Z., Lapolla, S.M., Plafker, S.M., Andrews, D.W., Lin, J., 2006. Auto-activation of the apoptosis protein Bax increases mitochondrial membrane permeability and is inhibited by Bcl-2. J. Biol. Chem. 281, 14764–14775.
Tjalkens, R.B., Zoran, M.J., Mohl, B., Barhoumi, R., 2006. Manganese suppresses ATP-dependent intercellular calcium waves in astrocyte networks through alteration of mitochondrial and endoplasmic reticulum calcium dynamics. Brain Res. 1113, 210–219.
Tomas-Camardiel, M., Herrera, A.J., Venero, J.L., Cruz Sanchez-Hidalgo, M., Cano, J., Machado, A., 2002. Differential regulation of glutamic acid decarboxylase mRNA and tyrosine hydroxylase mRNA expression in the aged manganese-treated rats. Brain Res. Mol. Brain Res. 103, 116–129.
Wedler, F.C., Ley, B.W., 1994. Kinetic, ESR, and trapping evidence for in vivo binding of Mn(II) to glutamine synthetase in brain cells. Neurochem. Res. 19, 139–144.
Werneburg, N.W., Guicciardi, M.E., Bronk, S.F., Kaufmann, S.H., Gores, G.J., 2007. Tumor necrosis factor-related apoptosis-inducing ligand activates a lysosomal pathway of apoptosis that is regulated by Bcl-2 proteins. J. Biol. Chem. 282, 28960–28970.
Yin, Z., Aschner, J.L., dos Santos, A.P., Aschner, M., 2008. Mitochondrial-dependent manganese neurotoxicity in rat primary astrocyte cultures. Brain Res. 1203, 1–11.
Yokel, R.A., 2006. Blood-brain barrier flux of aluminum, manganese, iron and other metals suspected to contribute to metal-induced neurodegeneration. J. Alzheimers Dis. 10, 223–253.